ACS OMEGA

Open Access

http://pubs.acs.org/journal/acsodf

Article

Dendrimer—Gold Nanocomposite-Based Electrochemical Aptasensor for the Detection of Dopamine

Dimpo S. Sipuka, Foluke O. G. Olorundare, Sesethu Makaluza, Nyasha Midzi, Tsholofelo I. Sebokolodi, Omotayo A. Arotiba,* and Duduzile Nkosi*

Cite This: *ACS Omega* 2023, 8, 33403−33411

Read Online

ACCESS | Metrics & More | Article Recommendations

ABSTRACT: Dopamine is an important neurotransmitter and biomarker that plays a vital role in our neurological system and body. Thus, it is important to monitor the concentration levels of dopamine in our bodies. We report an aptamer-based sensor fabricated through an electro-co-deposition of a generation 3 poly(propylene imine) (PPI) dendrimer and gold nanoparticles (AuNPs) on a glassy carbon (GC) electrode by cyclic voltammetry. Through self-assembly, a single-stranded thiolated dopamine aptamer was immobilized on the GC/PPI/AuNPs electrode to prepare an aptasensor. Voltammetry and electrochemical impedance spectroscopy (EIS) were used to characterize the modified electrodes. The readout for the biorecognition event between the aptamer and various dopamine concentrations was attained from square wave voltammetry and EIS. The aptasensor detected dopamine from the range of 10−200 nM, with a limit of detection of 0.26 and 0.011 nM from SWV and EIS, respectively. The aptasensor was selective toward dopamine when different amounts of epinephrine and ascorbic acid were present. The aptasensor was applicable in a more complex matrix of human serum.

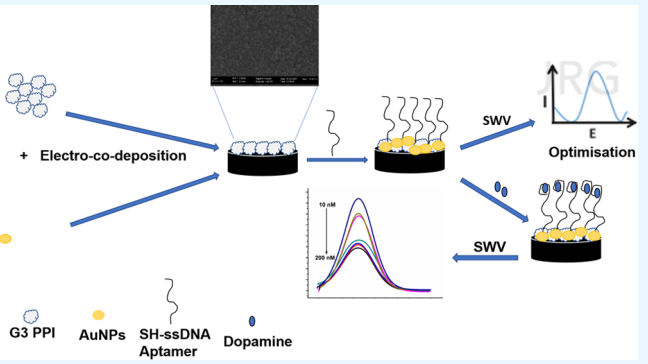

1. INTRODUCTION

Neurotransmitters are key messengers in the neurological system that serve a variety of functions. Dopamine is the most studied neurotransmitter. This is because of the critical role it plays in the human brain and neurological system.[1] Adrenal glands and several parts of the brain release dopamine. This neurotransmitter is essential for neuron development, attention, learning, and controlling stress reactions. The central nervous system, kidneys, hormones, motivational activities, and cardiovascular system are among its primary functions.[2] The functioning of the brain, feelings, and behavior of humans and animals is dependent on the concentration of dopamine. Parkinson's disease, schizophrenia, attention deficit hyperactivity disorder, and other diseases are said to be caused by abnormal amounts of dopamine concentrations.[2−4] These disorders are a result of damage to the involved neurons during the production of dopamine.

Various quantitative approaches, including electrophoresis, high liquid chromatography, and spectrophotometry, have been used to detect dopamine thus far. These methods can be expensive, and they necessitate time-consuming experiments.[5−7] Thus, researchers have been working on finding better methods of detecting dopamine sensitively and affordably in biological fluids. Electrochemical methods so far are preferred methods because of their ability to provide inexpensive, simple, and portable ways of detecting dopamine, as well as the fact that dopamine is a redox-active species allowing for the use of electrochemical methods.[8−13] The encountered challenge in using electrochemical methods for detecting dopamine is that the concentration of dopamine in physiological conditions is lower than that of the other electrochemically active species, such as ascorbic acid and uric acid.[14−16] Furthermore, these species, which also include epinephrine, norepinephrine, and catechol, are known as interfering species when it comes to detecting dopamine in biological samples since they have comparable oxidation potentials and competitive sensitivities. For example, ascorbic acid is commonly found to be a hundred to a thousand times greater than dopamine.[17−19] Thus, it is important to address the issue of selectivity in the development of sensors for dopamine.

Biosensor development is a viable strategy for the selective detection of dopamine. Biosensors are noted for their great

Received: May 6, 2023
Accepted: July 7, 2023
Published: September 5, 2023

selectivity and low detection limit. Thus, biosensors may mitigate the challenge of interferences from the biochemicals listed in the previous paragraph.[20−22] A biosensor usually needs a bioreceptor that undergoes a biorecognition process with the desired analyte. These bioreceptors can be enzymes, antibodies, DNA, RNA, and a whole cell. Certain DNA/RNA selected to bind to specific targets just as antibodies in immunosensors are called aptamers.[23] Aptamers are short single-stranded artificial ligands with strong affinity and specificity for their target molecule. These characteristics define the wide usage of aptamers in designing aptamer-based biosensors (also called aptasensors).[21,24] Aptamers possess key features, such as low cost, small size, simple synthesis, excellent recognition, and binding affinity with their target.[25,26] These features are an improvement over the traditional antibodies and can thus be exploited to improve the performance and selectivity of electrochemical biosensors.

Aptamers are usually immobilized on an electrode surface with the aid of a material or composite material that acts as a platform or immobilization layer. These immobilization layers, which can be in the nanodimension, assist in the performance of the biosensor. Nanomaterials on electrode surfaces or in electrochemical processes can increase electrocatalytic activities, increase electroactive surface area, and facilitate electron transfer.[27−30] Nanomaterials also provide a platform for the desired chemistry of immobilization, such as thiol linkage,[31] supramolecular interaction,[32] etc. Gold nanoparticles (AuNPs) have drawn a lot of interest from researchers due to their distinctive properties, including high biocompatibility, strong conductivity, and enhanced surface area.[33] AuNPs have been employed in detecting organic and inorganic pollutants, in biomedical applications, and as a nanoplatform for the construction of cancer biomarker immunosensors.[34,35] Another material of interest in biosensor development is poly(propylene imine) dendrimer and dendrimers in general. Poly(propylene imine) (PPI) dendrimers are globular-shaped, highly branching, three-dimensional polymers. These dendrimers possess numerous characteristics, which include biocompatibility, low cytotoxicity, solubility, self-assembly, and large surface area. Dendrimer's analytical properties enable them to be utilized in biological and materials science applications.[36,37]

Arotiba et al. have shown how dendrimer−gold nanocomposite may be used as a platform for DNA biosensor modification.[38] The use of this nanocomposite results in high conductivity and improved sensitivity of the sensor. Idris et al. used poly(propylene imine) dendrimer and gold nanoparticles when they developed an electrochemical immunosensor for cancer biomarkers.[39] While various electrochemical biosensors for detecting dopamine have been reported,[40−44] the use of dendrimers or dendrimer nanocomposites has not been reported. Owing to the host−guest potential of dendrimer and the immobilization chemistry such as thiol linkage that AuNPs can offer, an aptasensor for the detection of dopamine using PPI/AuNP nanocomposites is reported.

2. EXPERIMENTAL SECTION

2.1. Materials and Apparatus. A single-stranded DNA thiolated aptamer probe as reported in the literature with a sequence 5′-SH$(CH_2)_6$GTCTCTGTGTGCGCCAGAGACACTGGGGCAGATATGGGCCAGCACAGAATGAGGCCC-3′ [42] was purchased from Inqaba Biotechnical Industries (Pty) Ltd. (Pretoria, South Africa). Dopamine hydrochloride, epinephrine hydrochloride, potassium chloride, gold(III) chloride solution, G3 poly(propylene dendrimer) (G3 PPI), tris-(2-carboxyethyl) phosphine hydrochloride, ethylene diamine tetra-acetic acid (EDTA), tris-(hydroxymethyl) aminomethane, di-potassium hydrogen orthophosphate, potassium dihydrogen orthophosphate, and human serum (from human male AB plasma, USA origin, sterile-filtered) were purchased from Sigma-Aldrich (South Africa). To prepare 100 μM of aptamer, the purchased stock of the aptamer was dissolved using the Tris-EDTA buffer solution. The aptamer stock was stored at −20 °C. A 0.1 M phosphate buffer saline was prepared from dipotassium hydrogen orthophosphate and potassium dihydrogen orthophosphate. Ultrapure Millipore water was used for the preparation solutions (18.2 MΩ·cm at 25 °C, Millipore-MilliQ, South Africa).

2.2. Instrumentation. Electrochemical experiments and characterization were performed using an Ivium pocketstat2 potentiostat (Netherlands) connected to a three-electrode system. The three electrodes were the working electrode (glassy carbon), the reference electrode (Ag/AgCl in 3 M KCl), and the counter electrode (platinum wire). Field-emission scanning electron microscopy (FESEM) and transmission electron microscopy (TEM) analyses were conducted using an FESEM Zeiss crossbeam 540 and a Joel-TEM 2100F, respectively. UV−vis (Agilent Technologies Cary 60 UV−vis) was used for validation of the results from the sensor.

2.3. Preparation and Characterization of the Modified Electrode. PPI and gold nanoparticles were electro-co-deposited onto a glassy carbon (GC) electrode in a similar way to that reported by Arotiba et al.[38] Briefly, the GC electrode was cleaned with alumina slurry with different sizes (1.0, 0.3, and 0.05 μm), followed by sonication in deionized water and ethanol. The cleaned GC electrode was then modified using a solution of 5 mM G3 PPI and 5 mM gold(III) chloride in equal volumes. Using cycling voltammetry (CV), electro-co-deposition of PPI and AuNPs was carried out at a potential of −400 to 1000 mV for 10 cycles at a 50 mV/s scan rate. The obtained sensor was labeled GC/PPI/AuNPs.

The morphology of the AuNPs and generation 3 poly(propylene imine) (G3 PPI) dendrimer was investigated using field-emission scanning electron microscopy (FESEM). This analysis was carried out on a screen-printed carbon electrode. The nanomaterials were electrodeposited onto the carbon screen-printed electrode connected to a DropSens μStat 400 (Spain) using cyclic voltammetry. For this analysis, the working electrode was trimmed from the rest of the electrodes into a size of ≈1 cm^2. The stubs were then mounted on a FESEM stub holder, and an FESEM sputter was used to coat it with carbon. After coating, the stub holder was then placed on a stage of field-emission SEM, where the samples were analyzed by varying acceleration voltages.

Characterization of the electrodes was also carried out electrochemically using CV and electrochemical impedance spectroscopy (EIS). The conditions used at a potential window of −200 to 700 mV, 50 mV/s scan rate, and 10 mV E-step for CV. Electrochemical impedance spectroscopy (EIS) was conducted with a potential of 0.205 V, a frequency ranging from 100 kHz to 100 mHz, and an amplitude of 10 mV. The data were fitted using Randles's equivalent circuit. Electrodeposition of G3 PPI and AuNPs on the GC electrode was also carried out, and these electrodes were denoted as GC/PPI and GC/AuNPs.

https://doi.org/10.1021/acsomega.3c03133
ACS Omega 2023, 8, 33403−33411

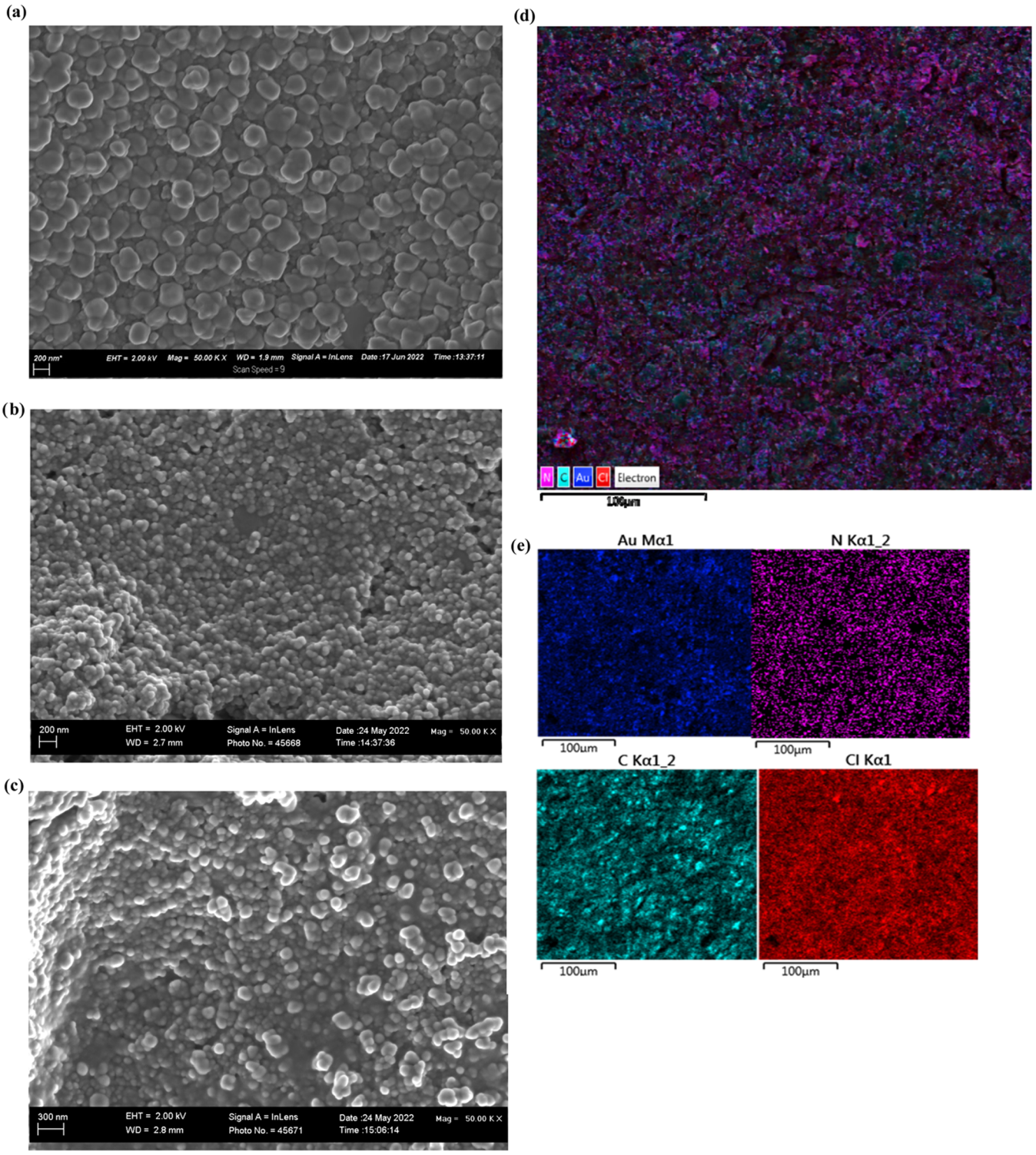

Figure 1. FESEM images on SPCE (a) AuNPs, (b) PPI, and (c) PPI/AuNPs. Elemental mapping: (d) all elements in the nanocomposite and (e) individual elements of the nanocomposite.

2.4. Preparation of the Dopamine Aptasensor. A 57 mer thiolated oligonucleotide (aptamer) for dopamine was immobilized on the GC/PPI/AuNPs. First, the aptamer solution was prepared by adding 1 mM tris(2-carboxyethyl) phosphine hydrochloride solution (TCEP) and was kept an hour in the dark for the reduction of disulfide bonds. After that, 10 μM of the aptamer probe was drop cast onto the GC/PPI/AuNPs and kept in a fridge at 4 °C overnight. The electrode was then rinsed using PBS to remove the unbound aptamers. The resultant electrode was GC/PPI/AuNPs-Apt.

3. RESULTS AND DISCUSSION

3.1. Physicochemical Characterization. The field-emission SEM images obtained for morphology studies are presented in Figure 1a–c. The gold nanoparticles (Figure 1a) appear as globular clusters, while G3 PPI appears as irregular

https://doi.org/10.1021/acsomega.3c03133
ACS Omega 2023, 8, 33403−33411

clusters or clumps of spheres and sheets on the electrode surface (Figure 1b). Figure 1c demonstrates a mixture of the dendrimer's larger cluster and the gold nanoparticle's globular clusters. Figure 1d,e presents the elemental mapping of PPI/AuNPs. The results show that PPI and AuNPs were uniformly distributed (Figure 1d) on the electrode based on the color code of the individual element (Figure 1e). The presence of chlorine might have emanated from the gold as our gold source was the gold(III) chloride solution.

3.2. Electrochemical Characterization of the Modified Glassy Carbon Electrode and the Aptasensor. The aptasensor (i.e., GC/PPI/AuNPs-Apt) was developed by the immobilization of the aptamer onto the GC/PPI/AuNPs electrode. Each component of the nanocomposite was used in the immobilization chemistry: the dendrimer provided a supramolecular anchor for the aptamer via host−guest chemistry and electrostatic attraction.[32,38,45] At pH of 7, the aptamer is anionic and the dendrimer is cationic, thus providing the electrostatic attraction.[46] The AuNPs, on the other hand, were used to anchor the thiolated aptamer through a gold−thiol linkage.[47−50] Cyclic voltammetry (CV) was performed to assess each phase of the modification using a redox probe (5 mM ferri/ferrocyanide—$[Fe(CN)_6]^{3-/4-}$). The responses of current for the bare glassy carbon (GC) electrode and those of the modified were observed. The aptasensor (i.e., GC/PPI/AuNPs-Apt) was prepared by the immobilization of the aptamer onto the GC/PPI/AuNPs electrode. The chemistry of immobilization is accomplished by a gold−thiol bond between the gold on the electrode's surface and the aptamer's thiol-modified end. Figure 2a represents the cyclic voltammograms. The G3 poly(propylene imine) dendrimer and gold nanoparticles (PPI/AuNPs)-modified electrode showed a much larger peak current response than the unmodified electrode (Figure 2a). The separation peak potential of the bare electrode is 0.17 V and that of the modified GC/PPI/AuNPs electrode is 0.09 V with an enhanced peak current. The increase of the peak current resulted from the co-electrodeposition of the nanomaterials as they possess excellent characteristics, such as biocompatibility, facile electron transfer, and improved electroactive surface area.[51] Nevertheless, following the aptamer's immobilization on the GC/PPI/AuNPs electrode, a reduction in peak current was observed. This decrease is brought about by the repulsion of charge between the aptamer (due to its negatively charged sugar-phosphate backbone) and the anionic ferri/ferrocyanide that blocks electron flow to the electrode's surface. This reduced current confirmed the immobilization of the aptamer.[31]

From Figure 2a, the peak current was maximum at the GC/PPI/AuNPs surface. The synergic effect is due to the increased electrooxidation current as the result of the enormous surface area and conductivity of the AuNPs. PPI is cationic and thus presents the possibility of adding electrostatic attraction to the mechanism through which the ferri/ferricyanide (FC) diffuses to the electrode surface. Thus, more FC are attracted or present at the interface per unit time leading to a higher current.

Furthermore, the scan rate study (Figure 2b) reveals a linear relationship between the anodic peak current and the square root of the scan rate (Figure 2b inset) with a correlation coefficient of R^2 = 0.9968 for the GC/PPI/AuNPs. These findings suggest that diffusion controls the electrochemical response. The surface area of GC/PPI/AuNPs was modified,

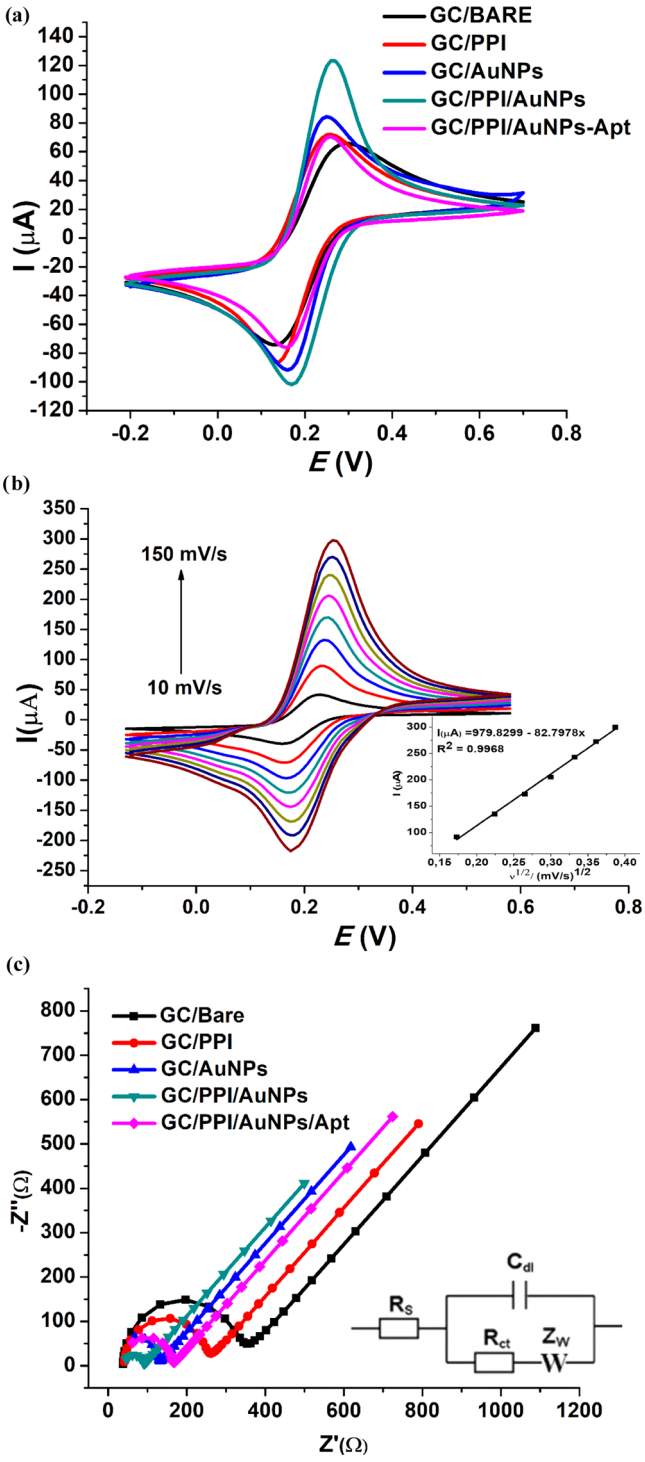

Figure 2. (a) CV: bare and modified GC electrodes at 50 mV/s scan rate and (b) scan rate study of the GC/PPI/AuNPs electrode, (c) The EIS responses−Nyquist plot (bare and modified), Inset: Randles equivalent circuit. The experiments were carried out using 5 mM ferri/ferrocyanide in 0.1 M PBS, pH 7.4.

and the bare was determined using the Randles−Sevcik equation. The bare electrode's surface area was determined to be 0.059 cm^2, whereas the GC/PPI/AuNPs was 0.265 cm^2. From these results, it can be observed that the properties of the dendrimer−gold nanocomposite functioned in synergy in improving the electrode's electroactive surface area. Furthermore, the scan rate study shows the stability of the

https://doi.org/10.1021/acsomega.3c03133
ACS Omega 2023, 8, 33403−33411

Scheme 1. Schematic Representation of the Aptasensor Development

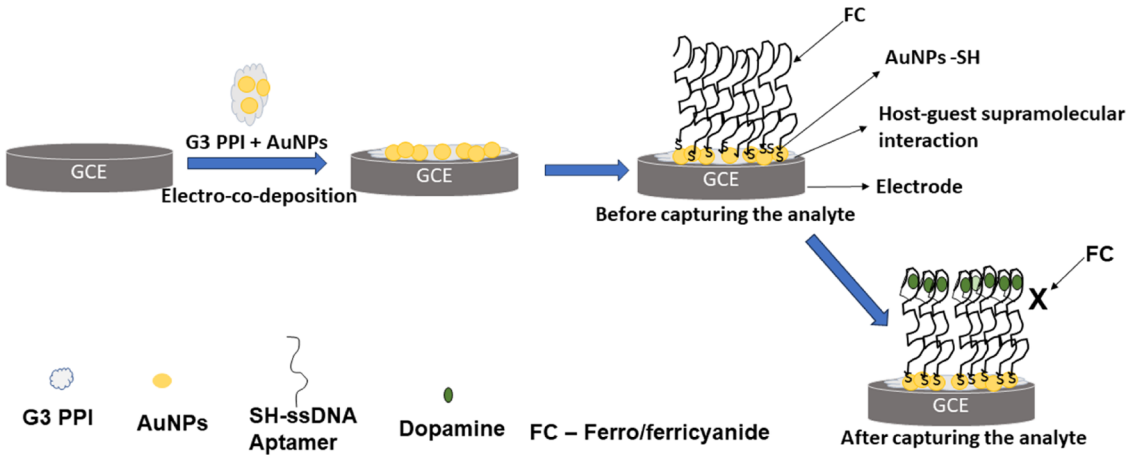

electrodeposited PPI/AuNPs because the anodic and cathodic potential did not vary as the scan rate changed.[39] This stability is because of the electrodeposition method used for PPI and AuNPs. For PPI, the electrodeposition involves a stable C−N linkage on the electrode surface. This CN linkage further traps the AuNP within the dendrimer network.[38] Gold nanoparticles also have excellent stability due to their chemical and physical properties.[52]

The electrodes were also characterized by electrochemical impedance spectroscopy. Data from the Nyquist plot was fitted using the Randles equivalent circuit (Figure 2c, inset), which consists of solution resistance (R_s), charge transfer resistance (R_{ct}), Warburg impedance (Z_w), and double-layer capacitance (C) (Figure 2c). The values of the charge transfer resistance (R_{ct}) for the electrodes are 289, 205, 117, and 35 Ω for the bare GC, GC/PPI, GC/AuNPs, and GC/PPI/AuNPs, respectively. The decrease in R_{ct} values as the electrode was modified with PPI and AuNPs indicated that these nanomaterials can facilitate electron transfer. The GC/PPI/AuNPs electrode has the lowest R_{ct} value of 35 Ω. This indicates that the electro-co-deposited nanocomposite of PPI and AuNPs has a combined effect that outweighs each individual in contributing to the improvement of the electron transfer of the redox probe at the electrode interface. Upon immobilization of the dopamine aptamer, an R_{ct} value of 127 Ω was obtained, showing that the introduction of the aptamer hindered electron flow. The results obtained from impedance spectroscopy for the electrodes agree with that obtained from CV (Figure 2a). Scheme 1 summerizes the aptasensor design and its detection mechanism.

3.3. Optimization of Experimental Parameters. When developing the biosensor, square wave voltammetry (SWV) was utilized to optimize the experimental parameters, including the aptamer concentration and the incubation duration. The aptamer concentration was varied from 1 to 15 μM and was drop cast onto the modified GC/PPI/AuNPs electrode. The current increase was noted to increase with the increase in aptamer concentration until the concentration reached 10 μM and then it decreased, as seen in Figure 3a. Thus, the optimum concentration was 10 μM for the experiments. The impact of incubation time on the sensitivity of the aptasensor was also studied from 5 to 240 min. As depicted in Figure 3b, the current was the highest during the first 30 min of incubation, then the current decreased at about 60 min and slightly

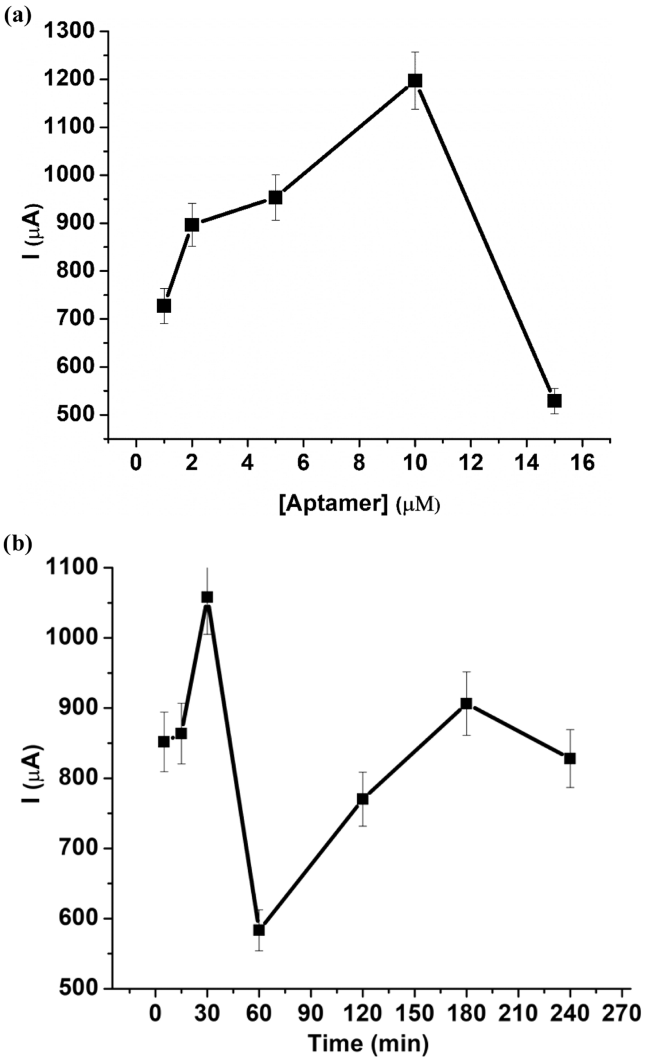

Figure 3. SWV responses: (a) different aptamer concentrations and (b) aptamer incubation time. The experiments were carried out using 5 mM ferri/ferrocyanide in 0.1 M PBS, pH 7.4.

increased after that but still less than the 30 min. Thus, the optimal incubation time for the aptamer was 30 min.

3.4. Analytical Performance of the Aptamer-based Sensor. SWV and EIS were used for the detection of

https://doi.org/10.1021/acsomega.3c03133
ACS Omega 2023, 8, 33403−33411

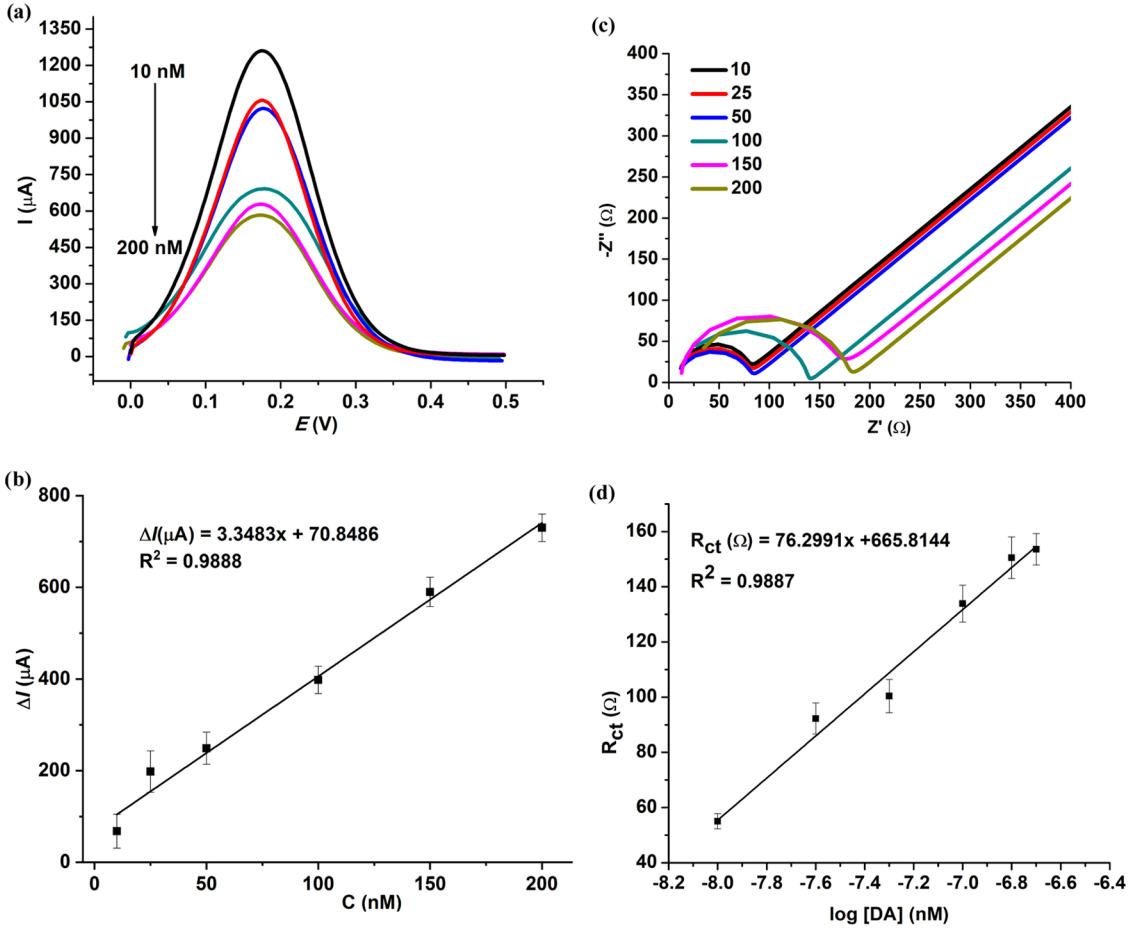

Figure 4. (a) SWV responses of aptasensor-to-dopamine concentrations, (b) calibration plot of SWV responses, (c) Nyquist plots of the biosensor from different concentrations of dopamine, and (d) calibration plot of the EIS responses. The experiments were carried out using 5 mM ferri/ferrocyanide in 0.1 M PBS, pH 7.4.

Table 1. Comparison of Biosensors for the Detection of Dopamine[a]

electrode material	method	detection limit	linear range	refs
AuE-DNA DA aptamer	SWV	0.001 μM	0.005−0.15 μM	53
Au-SPE DA aptamer	CV and EIS	60 and 90 pM	10−0.1 nM	54
AuE-gold nanostructure	DPV	0.01 nM	0.163−20 nM	10
Cr-JFC/DAC_2	DPV	10.6 nM	0.05−4 μM	55
GCE-rGRO-AuNPs	DPV	0.13 μM	0.5−20 μM	11
Tyr@PANI/CNTs/CNC	CV	1.57 nM	7−1000 mM	56
PANi/CQDs	CV	0.1013 μM	10−90 μM	44
GCE/PPI/AuNPs	SWV	0.26 nM	10−200 nM	this work
GCE/PPI/AuNPs	EIS	0.011 nM	10−200 nM	this work

[a]GCE, glassy carbon electrode; PANi/CQDS, polyaniline/carbon quantum dots; AuE, gold electrode; Au-SPE, Gold screen-printed electrode, rGRO-AuNPs, reduced graphene oxide-gold nanoparticle; Tyr@PANI/CNTs/CNC, Tyr immobilized polyaniline/carbon nanotubes/cellulose nanocrystals.

dopamine by the aptasensor at optimized conditions. The current responses (from SWV) decreased as dopamine concentrations increased from 10 to 200 nM (Figure 4a). Change in peak current was determined using $\Delta I_p = I_0 - I$, where I is the anodic peak current after dopamine incubation and I_0 is the anodic peak current before dopamine incubation. The calibration curve has a linear regression equation of $\Delta I(\mu A) = 3.3483x + 70.8486$ with a correlation coefficient of $R^2 = 0.9888$ for SWV (Figure 4b). EIS was also used to interrogate the biosensing of dopamine (Figure 4c). In this case, the charge transfer resistance (R_{ct}) increased with increasing concentration of dopamine. The binding of dopamine by the aptamer results in the folding of the aptamer around the target. The folding at the aptasensor surface (as more dopamine is bound) repels the interfacial electron transfer of the ferri/ferrocyanide redox probe, leading to an increase in R_{ct} (Scheme 1). The calibration plot (Figure 4d) has a linear regression equation of R_{ct} (Ω) = 76.2991x + 665.8144 for EIS with $R^2 = 0.9887$. The detection limits from SWV and EIS were determined with the use of this equation $\frac{3 \times SD}{slope}$, SD is the standard deviation of the blank solution in

https://doi.org/10.1021/acsomega.3c03133
ACS Omega 2023, 8, 33403−33411

three replicates and the slope is that of the calibration curve. The calculated detection limits were 0.26 and 0.011 nM for SWV and EIS, respectively. The obtained detection limits and linear range obtained in this work are comparable (in some cases better) with other reported biosensors for the detection of dopamine as shown in Table 1.

3.5. Selectivity, Reproducibility, and Stability of the Biosensor. The selectivity of the aptasensor was probed with interfering species, such as epinephrine and ascorbic acid. The findings indicate that the sensor could detect dopamine (50 nM) in the presence of epinephrine and ascorbic acid even though their concentrations at 100 and 200 nM were greater than that of dopamine (Figure 5a). The results suggest that the aptasensor is selective when the interfering molecules are present.

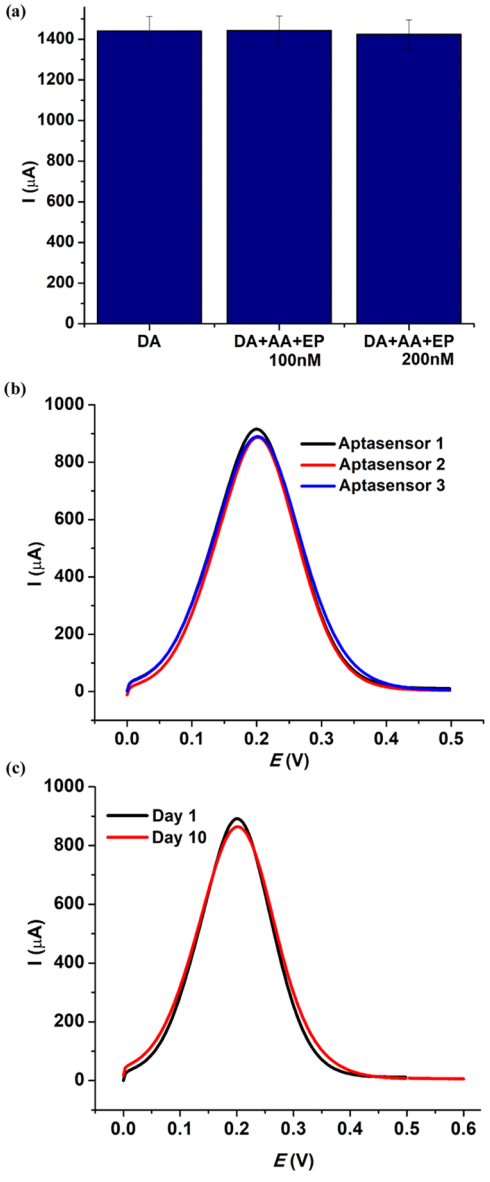

Figure 5. (a) Selectivity of the aptasensor to 50 nM dopamine, 50 nM DA, and 100 nM epinephrine and ascorbic acid, 50 nM DA and 200 nM epinephrine and ascorbic acid. (b) Reproducibility investigation of the aptasensor. (c) Stability study of the aptasensor to 10 nM dopamine.

To study the reproducibility of the biosensor, three biosensors of different electrodes in 10 nM dopamine were used. The % relative standard deviation (% RSD) for three measures of dopamine using the same biosensor was calculated to be 1.3%. The % RSD with three different aptasensors was 2.21% (Figure 5b). The results demonstrated good reproducibility of the biosensor. To study the stability of the as-prepared biosensor, it was then prepared using the same way and was used to detect the same concentration of dopamine after which it was stored at 4 °C in a refrigerator for 10 days (Figure 5c).

3.6. Application of the Biosensor in Real Sample Analysis. The practical applicability of the biosensor was carried out by detecting dopamine in the human serum sample. The samples were diluted with the PBS solution, and then, various concentrations of dopamine were added (10 and 20 nM). The results were validated using UV−vis, and the recoveries were 103.5 and 121% (Table 2). These results show that the developed biosensor can detect dopamine.

Table 2. Analysis of Dopamine in Human Serum

sample	spike (nM)	found (nM)	found UV−vis (nM)	recovery %
human serum	0	101.0	108.2	
	10	113.1	119.2	121
	20	121.7	127.1	103.5

4. CONCLUSIONS

A dendrimer−gold nanocomposite-based aptasensor for dopamine was developed. While the aptamer was linked to the electrode surface by the Au−SH linkage, the immobilization was further improved by the supramolecular interaction of the PPI dendrimer owing to its host−guest capability. This nanocomposite platform can thus be extended to the immobilization of other bioreceptors. Furthermore, the preparation of this aptasensor is a simple, easily controlled electro-co-deposition step. The deposition approach is better than multiple steps of electrode preparation and drop coating usually reported for sensor preparation. The synergic effect of the nanomaterials used enhanced the sensitivity of the aptasensor toward the detection of dopamine. The aptasensor showed stability, reproducibility, and selectivity in detecting DA in the presence of epinephrine and ascorbic acid as interfering molecules. Both SWV and EIS can be used to read out the biorecognition of the aptamer with the dopamine molecules. The limits of detection of 0.26 and 0.011 nM dopamine were calculated for SWV and EIS, respectively. These limits of detection fall below many reports in the literature. An aspect to improve, however, is to apply the sensor measurement in phosphate buffer rather than in the ferrocyanide redox probe. The use of phosphate buffer will make the measurement more direct (signal on). The aptasensor detected dopamine in human serum samples, denoting its potential for practical application.

AUTHOR INFORMATION

Corresponding Authors

Omotayo A. Arotiba − *Department of Chemical Sciences, University of Johannesburg, 2028 Johannesburg, South Africa; Centre for Nanomaterials Science Research, University of Johannesburg, 2028 Johannesburg, South Africa;*

https://doi.org/10.1021/acsomega.3c03133
ACS Omega 2023, 8, 33403−33411

orcid.org/0000-0002-8227-8684; Email: oarotiba@uj.ac.za

Duduzile Nkosi − *Department of Chemical Sciences, University of Johannesburg, 2028 Johannesburg, South Africa*; Email: dnkosi@uj.ac.za

Authors

Dimpo S. Sipuka − *Department of Chemical Sciences, University of Johannesburg, 2028 Johannesburg, South Africa; Centre for Nanomaterials Science Research, University of Johannesburg, 2028 Johannesburg, South Africa*

Foluke O. G. Olorundare − *Department of Chemical Sciences, University of Johannesburg, 2028 Johannesburg, South Africa*

Sesethu Makaluza − *Department of Chemical Sciences, University of Johannesburg, 2028 Johannesburg, South Africa; Centre for Nanomaterials Science Research, University of Johannesburg, 2028 Johannesburg, South Africa*

Nyasha Midzi − *Department of Chemical Sciences, University of Johannesburg, 2028 Johannesburg, South Africa*

Tsholofelo I. Sebokolodi − *Department of Chemical Sciences, University of Johannesburg, 2028 Johannesburg, South Africa; Centre for Nanomaterials Science Research, University of Johannesburg, 2028 Johannesburg, South Africa*

Complete contact information is available at: https://pubs.acs.org/10.1021/acsomega.3c03133

Notes

The authors declare no competing financial interest.

■ ACKNOWLEDGMENTS

This research study was financially supported by the National Research Foundation, South Africa (CPRR Grant No. 118546 (Author O.A.A.) and CSUR Grant No. 129396 (Author D.N.)), and the Centre for Nanomaterials Science Research (University of Johannesburg).

■ REFERENCES

(1) Matt, S. M.; Gaskill, P. J. Where Is Dopamine and How Do Immune Cells See It?: Dopamine-Mediated Immune Cell Function in Health and Disease. *J. Neuroimmune Pharmacol.* **2020**, *15*, 114−164.

(2) Meng, L.; Wang, M.; Gao, Y.; Chen, L.; Wang, K.; Gao, W.; Liu, Q. Dopamine D1 Receptor Agonist Alleviates Acute Lung Injury via Modulating Inflammatory Responses in Macrophages and Barrier Function in Airway Epithelial Cells. *Free Radical Biol. Med.* **2023**, *202*, 2−16.

(3) Shen, T.; Pu, J. L.; Jiang, Y. S.; Yue, Y. M.; He, T. T.; Qu, B. Y.; Zhao, S.; Yan, Y. P.; Lai, H. Y.; Zhang, B. R. Impact of Cognition-Related Single Nucleotide Polymorphisms on Brain Imaging Phenotype in Parkinson's Disease. *Neural Regener. Res.* **2023**, *18*, 1154−1160.

(4) Klein, M. O.; Battagello, D. S.; Cardoso, A. R.; Hauser, D. N.; Bittencourt, J. C.; Correa, R. G. Dopamine: Functions, Signaling, and Association with Neurological Diseases. *Cell. Mol. Neurobiol.* **2019**, *39*, 31−59.

(5) Tang, J.; Jiang, S.; Liu, Y.; Zheng, S.; Bai, L.; Guo, J.; Wang, J. Electrochemical Determination of Dopamine and Uric Acid Using a Glassy Carbon Electrode Modified with a Composite Consisting of a Co(II)-Based Metalorganic Framework (ZIF-67) and Graphene Oxide. *Microchim. Acta* **2018**, *185*, No. 486.

(6) Bashar, F.; Eddin, K. Recent Advances in Electrochemical and Optical Sensing of Dopamine. *Sensors* **2020**, *20*, No. 1039.

(7) Ma, B.; Guo, H.; Wang, M.; Li, L.; Jia, X.; Chen, H.; Xue, R.; Yang, W. Electrocatalysis of Cu−MOF/Graphene Composite and Its Sensing Application for Electrochemical Simultaneous Determination of Dopamine and Paracetamol. *Electroanalysis* **2019**, *31*, 1002−1008.

(8) Shimna, T.; Thomas, J.; Thomas, T.; Thomas, N. Porous Co3O4 Modified Carbon Paste Electrode for the Quantification of Dopamine. *J. Appl. Electrochem.* **2020**, *50*, 1165−1173.

(9) Lu, Z.; Li, Y.; Liu, T.; Wang, G.; Sun, M.; Jiang, Y.; He, H.; Wang, Y.; Zou, P.; Wang, X.; Zhao, Q.; Rao, H. A Dual-Template Imprinted Polymer Electrochemical Sensor Based on AuNPs and Nitrogen-Doped Graphene Oxide Quantum Dots Coated on NiS2/Biomass Carbon for Simultaneous Determination of Dopamine and Chlorpromazine. *Chem. Eng. J.* **2020**, *389*, No. 124417.

(10) Taheri, R. A.; Eskandari, K.; Negahdary, M. An Electrochemical Dopamine Aptasensor Using the Modified Au Electrode with Spindle-Shaped Gold Nanostructure. *Microchem. J.* **2018**, *143*, 243−251.

(11) Chen, T.; Tang, L.; Yang, F.; Zhao, Q.; Jin, X.; Ning, Y.; Zhang, G. J. Electrochemical Determination of Dopamine by a Reduced Graphene Oxide−Gold Nanoparticle-Modified Glassy Carbon Electrode. *Anal. Lett.* **2016**, *49*, 2223−2233.

(12) Terán-Alcocer, Á.; Bravo-plascencia, F.; Cevallos-morillo, C.; Palma-cando, A. Electrochemical Sensors Based on Conducting Polymers for the Aqueous Detection of Biologically Relevant Molecules. *Nanomaterials* **2021**, *11*, No. 252.

(13) Benvidi, A.; Dehghani-Firouzabadi, A.; Mazloum-Ardakani, M.; Mirjalili, B. B. F.; Zare, R. Electrochemical Deposition of Gold Nanoparticles on Reduced Graphene Oxide Modified Glassy Carbon Electrode for Simultaneous Determination of Levodopa, Uric Acid and Folic Acid. *J. Electroanal. Chem.* **2015**, *736*, 22−29.

(14) Selvolini, G.; Lazzarini, C.; Marrazza, G. Electrochemical Nanocomposite Single-Use Sensor for Dopamine Detection. *Sensors* **2019**, *19*, No. 3097.

(15) Sajid, M.; Nazal, M. K.; Mansha, M.; Alsharaa, A.; Jillani, S. M. S.; Basheer, C. Chemically Modified Electrodes for Electrochemical Detection of Dopamine in the Presence of Uric Acid and Ascorbic Acid: A Review. *TrAC, Trends Anal. Chem.* **2016**, *76*, 15−29.

(16) Chen, Y.; Li, X.; Cai, G.; Li, M.; Tang, D. In Situ Formation of (0 0 1)TiO2/Ti3C2 Heterojunctions for Enhanced Photoelectrochemical Detection of Dopamine. *Electrochem. Commun.* **2021**, *125*, No. 106987.

(17) Vilian, A. T. E.; Rajkumar, M.; Chen, S.-M. In Situ Electrochemical Synthesis of Highly Loaded Zirconium Nanoparticles Decorated Reduced Graphene Oxide for the Selective Determination of Dopamine and Paracetamol in Presence of Ascorbic Acid.Pdf. *Colloids Surf., B* **2014**, *115*, 295−301.

(18) Patella, B.; Sortino, A.; Mazzara, F.; Aiello, G.; Drago, G.; Torino, C.; Vilasi, A.; O'Riordan, A.; Inguanta, R. Electrochemical Detection of Dopamine with Negligible Interference from Ascorbic and Uric Acid by Means of Reduced Graphene Oxide and Metals-NPs Based Electrodes. *Anal. Chim. Acta* **2021**, *1187*, No. 339124.

(19) Li, R.; Liang, H.; Zhu, M.; Lai, M.; Wang, S.; Zhang, H.; Ye, H.; Zhu, R.; Zhang, W. Electrochemical Dual Signal Sensing Platform for the Simultaneous Determination of Dopamine, Uric Acid and Glucose Based on Copper and Cerium Bimetallic Carbon Nanocomposites. *Bioelectrochemistry* **2021**, *139*, No. 107745.

(20) Phumlani, T.; Shumbula, P. M.; Njengele-Tetyana, Z. Biosensors: Design, Development and Applications. In *Nanopores*; Ameen, S.; Shaheer, A. M.; Shin, H.-S., Eds.; IntechOpen, 2021; Vol. *11*, pp 1−19.

(21) Ni, S.; Zhuo, Z.; Pan, Y.; Yu, Y.; Li, F.; Liu, J.; Wang, L.; Wu, X.; Li, D.; Wan, Y.; Zhang, L.; Yang, Z.; Zhang, B.; Lu, A.; Zhang, G. Recent Progress in Aptamer Discoveries and Modifications for Therapeutic Applications. *ACS Appl. Mater. Interfaces* **2021**, *13*, 9500−9519.

(22) Li, Y.; Zeng, R.; Wang, W.; Xu, J.; Gong, H.; Li, L.; Li, M.; Tang, D. Size-Controlled Engineering Photoelectrochemical Biosensor for Human Papillomavirus-16 Based on CRISPR-Cas12a-Induced Disassembly of Z-Scheme Heterojunctions. *ACS Sens.* **2022**, *7*, 1593−1601.

(23) Qiu, Z.; Shu, J.; Liu, J.; Tang, D. Dual-Channel Photoelectrochemical Ratiometric Aptasensor with up-Converting Nanocrystals Using Spatial-Resolved Technique on Homemade 3D Printed Device. *Anal. Chem.* **2019**, *91*, 1260−1268.

(24) Malvano, F.; Albanese, D.; Pilloton, R.; Di, M. A New Label-Free Impedimetric Aptasensor for Gluten Detection. *Food Control* **2017**, *79*, 200−206.
(25) Li, Z.; Mohamed, M. A.; Vinu Mohan, A. M.; Zhu, Z.; Sharma, V.; Mishra, G. K.; Mishra, R. K. Application of Electrochemical Aptasensors toward Clinical Diagnostics, Food, and Environmental Monitoring: Review. *Sensors* **2019**, No. 5435.
(26) Xu, Y.; Cheng, G.; He, P.; Fang, Y. A Review: Electrochemical Aptasensors with Various Detection Strategies. *Electroanalysis* **2009**, *21*, 1251−1259.
(27) Evtugyn, G.; Porfireva, A.; Shamagsumova, R.; Hianik, T. Advances in Electrochemical Aptasensors Based on Carbon Nanomaterials. *Chemosensors* **2020**, *8*, No. 96.
(28) Idris, A. O.; Mogamisi, N. K.; Mtunzi, F.; Arotiba, O. A. Poly (Propylene Imine) Coated Gold Nanoparticles Sensor for Cd (II) in Water. *Eurasian J. Anal. Chem.* **2021**, *16*, No. 122641.
(29) Lakard, S.; Pavel, I.; Lakard, B. Electrochemical Biosensing of Dopamine Neurotransmitter: A Review. *Biosensors* **2021**, *11*, No. 179.
(30) Mokwebo, K. V.; Oluwafemi, O. S.; Arotiba, O. A. An Electrochemical Cholesterol Biosensor Based on A CdTe/CdSe/ZnSe Quantum Dots—Poly (Propylene Imine) Dendrimer Nanocomposite Immobilisation Layer. *Sensors* **2018**, *18*, No. 3368.
(31) Mushiana, T.; Mabuba, N.; Idris, A. O.; Peleyeju, G. M.; Orimolade, B. O.; Nkosi, D.; Ajayi, R. F.; Arotiba, O. A. An Aptasensor for Arsenic on a Carbon-gold Bi-Nanoparticle Platform. *Sens. Bio-Sensing Res.* **2019**, *24*, No. 100280.
(32) Soda, N.; Arotiba, O. A. An Electrochemical Aptasensor for Thrombin Based on a Novel Polyamidoamine Dendrimer-Streptavidin Supramolecular Architecture. *Int. J. Electrochem. Sci.* **2017**, *12*, 10359−10368.
(33) Xiao, T.; Huang, J.; Wang, D.; Meng, T.; Yang, X. Au and Au-Based Nanomaterials: Synthesis and Recent Progress in Electrochemical Sensor Applications. *Talanta* **2020**, *206*, No. 120210.
(34) Pilehvar, S.; Reinemann, C.; Bottari, F.; Vanderleyden, E.; Van Vlierberghe, S.; Blust, R.; Strehlitz, B.; De Wael, K. A Joint Action of Aptamers and Gold Nanoparticles Chemically Trapped on a Glassy Carbon Support for the Electrochemical Sensing of Ofloxacin. *Sensors Actuators, B Chem.* **2017**, *240*, 1024−1035.
(35) Idris, A. O.; Mabuba, N.; Arotiba, O. A. An Exfoliated Graphite-Based Electrochemical Immunosensor on a Dendrimer/Carbon Nanodot Platform for the Detection of Carcinoembryonic Antigen Cancer Biomarker. *Biosensors* **2019**, *9*, No. 39.
(36) Idris, A. O.; Mamba, B.; Feleni, U. Poly (Propylene Imine) Dendrimer: A Potential Nanomaterial for Electrochemical Application. *Mater. Chem. Phys.* **2020**, *244*, No. 122641.
(37) Arotiba, O. A.; Baker, P. G.; Mamba, B. B.; Iwuoha, E. I. The Application of Electrodeposited Poly (Propylene Imine) Dendrimer as an Immobilisation Layer in a Simple Electrochemical DNA Biosensor. *Int. J. Electrochem. Sci.* **2011**, *6*, 673−683.
(38) Arotiba, O.; Owino, J.; Songa, E.; Hendricks, N.; Waryo, T.; et al. An Electrochemical DNA Biosensor Developed on a Nanocomposite Platform of Gold and Poly(Propyleneimine) Dendrimer. *Sensors* **2008**, *8*, 6791−6809.
(39) Idris, A. O.; Mabuba, N.; Arotiba, O. A. A Dendrimer Supported Electrochemical Immunosensor for the Detection of Alpha-Feto Protein − a Cancer Biomarker. *Electroanalysis* **2018**, *30*, 31−37.
(40) Álvarez-Martos, I.; Ferapontova, E. E. Electrochemical Label-Free Aptasensor for Specific Analysis of Dopamine in Serum in the Presence of Structurally Related Neurotransmitters. *Anal. Chem.* **2016**, *88*, 3608−3616.
(41) Bahrami, S.; Abbasi, A. R.; Roushani, M.; Derikvand, Z.; Azadbakht, A. An Electrochemical Dopamine Aptasensor Incorporating Silver Nanoparticle, Functionalized Carbon Nanotubes and Graphene Oxide for Signal Amplification. *Talanta* **2016**, *159*, 307−316.
(42) Ahmed, J.; Faisal, M.; Harraz, F. A.; Jalalah, M.; Alsareii, S. A. Development of an Amperometric Biosensor for Dopamine Using Novel Mesoporous Silicon Nanoparticles Fabricated via a Facile Stain Etching Approach. *Phys. E* **2022**, *135*, No. 114952.
(43) Guo, T.; Wu, C.; Offenhäusser, A.; Mayer, D. A Novel Ratiometric Electrochemical Biosensor Based on a Split Aptamer for the Detection of Dopamine with Logic Gate Operations. *Phys. Status Solidi A* **2020**, *217*, No. 1900924.
(44) Ratlam, C.; Phanichphant, S.; Sriwichai, S. Development of Dopamine Biosensor Based on Polyaniline/Carbon Quantum Dots Composite. *J. Polym. Res.* **2020**, *27*, No. 183.
(45) Tsekeli, T. R.; Sebokolodi, T. I.; Sipuka, D. S.; Olorundare, F. O. G.; Akanji, S. P.; Nkosi, D.; Arotiba, O. A. A Poly (Propylene Imine) Dendrimer − Carbon Nanofiber Based Aptasensor for Bisphenol A in Water. *J. Electroanal. Chem.* **2021**, *901*, No. 115783.
(46) John, S. V.; Rotherham, L. S.; Khati, M.; Mamba, B. B.; Arotiba, O. A. Towards HIV Detection: Novel Poly(Propylene Imine) Dendrimer-Streptavidin Platform for Electrochemical DNA and Gp120 Aptamer Biosensors. *Int. J. Electrochem. Sci.* **2014**, *9*, 5425−5437.
(47) Talemi, R. P.; Mousavi, S. M.; Afruzi, H. Using Gold Nanostars Modified Pencil Graphite Electrode as a Novel Substrate for Design a Sensitive and Selective Dopamine Aptasensor. *Mater. Sci. Eng. C* **2017**, *73*, 700−708.
(48) Liu, L.; Xia, N.; Meng, J. J.; Zhou, B. Bin.; Li, S. J. An Electrochemical Aptasensor for Sensitive and Selective Detection of Dopamine Based on Signal Amplification of Electrochemical-Chemical Redox Cycling. *J. Electroanal. Chem.* **2016**, *775*, 58−63.
(49) Girolamo, A. De.; Mckeague, M.; Pascale, M. Immobilization of Aptamers on Substrates. In *Aptamers for Analytical Applications: Affinity Acquisition and Method Design*; Dong, Y., Ed.; Wiley-VCHVerlag GmbH & Co. KGaA, 2018; pp 85−126.
(50) Zhuang, J.; Lai, W.; Xu, M.; Zhou, Q.; Tang, D. Plasmonic AuNP/g-C3N4 Nanohybrid-Based Photoelectrochemical Sensing Platform for Ultrasensitive Monitoring of Polynucleotide Kinase Activity Accompanying Dnazyme-Catalyzed Precipitation Amplification. *ACS Appl. Mater. Interfaces* **2015**, *7*, 8330−8338.
(51) Ndlovu, T.; Arotiba, O. A. Poly(Propylene Imine) Dendrimer and Gold Nanoparticles as Anti-Passivating Electrode Modifiers in Phenol Sensing - A Case Study of 4-Chorophenol. *Int. J. Electrochem. Sci.* **2015**, *10*, 8224−8235.
(52) Sipuka, D. S.; Sebokolodi, T. I.; Olorundare, F. O. G.; Muzenda, C.; Nkwachukwu, O. V.; Nkosi, D.; Arotiba, O. A. Electrochemical Sensing of Epinephrine on a Carbon Nanofibers and Gold Nanoparticle-Modified Electrode. *Electrocatalysis* **2023**, *14*, 9−17.
(53) Zhou, J.; Wang, W.; Yu, P.; Xiong, E.; Zhang, X.; Chen, J. A Simple Label-Free Electrochemical Aptasensor for Dopamine Detection. *RSC Adv.* **2014**, *4*, 52250−52255.
(54) Abu-ali, H.; Ozkaya, C.; Davis, F.; Walch, N.; Nabok, A. Electrochemical Aptasensor for Detection of Dopamine. *Chemosensors* **2020**, *8*, No. 28.
(55) Gong, W.; Li, J.; Chu, Z.; Yang, D.; Subhan, S.; Li, J.; Huang, M.; Zhang, H.; Zhao, Z. A Low-Cost High-Entropy Porous CrO/CrN/C Biosensor for Highly Sensitive Simultaneous Detection of Dopamine and Uric Acid. *Microchem. J.* **2022**, *175*, No. 107188.
(56) Dhanjai; Yu, N.; Mugo, S. M. Disposable Capacitive Biosensor for Dopamine Sensing. *ChemistrySelect* **2020**, *5*, 12470−12476.

https://doi.org/10.1021/acsomega.3c03133
ACS Omega 2023, 8, 33403−33411